



Ballester-Beltrán, J., Lebourg, M., Rico, P., and Salmeron-Sanchez, M. (2015) Cell migration within confined sandwich-like nanoenvironments. *Nanomedicine*, 10(5), pp. 815-828.

Copyright © 2015 Future Medicine Ltd.

A copy can be downloaded for personal non-commercial research or study, without prior permission or charge

Content must not be changed in any way or reproduced in any format or medium without the formal permission of the copyright holder(s)

When referring to this work, full bibliographic details must be given

<http://eprints.gla.ac.uk/103606>

Deposited on: 27 April 2015

Enlighten – Research publications by members of the University of Glasgow_
<http://eprints.gla.ac.uk>

1 Cell migration within confined sandwich-like nanoenvironments

2

3 Abstract

4 **Aim:** We introduced sandwich-like cultures to provide cell migration studies with
5 representative nano-bio-environments where both ventral and dorsal cell receptors are
6 activated. **Methods:** We have investigated different nano-environmental conditions by
7 changing the protein coating (fibronectin, vitronectin) and/or materials (using polymers
8 that adsorb proteins in qualitatively different conformations) of this sandwich system to
9 show their specific role in cell migration. **Results:** Here we show that cell migration
10 within sandwich cultures greatly differs from 2D cultures and shares some similarities
11 with migration within 3D environments. Beyond differences in cell morphology and
12 migration, dorsal stimulation promotes cell remodeling of the ECM over simple ventral
13 receptor activation in traditional 2D cultures.

14

15 **Keywords:** sandwich culture, 3D cell migration, cell motility, lobopodia-based
16 migration, fibronectin

17

18

19

20

21

22 **Introduction**

23 Cell migration is an essential process from embryonic development to adulthood.
24 Hence, studying cell migration on well-defined nano-bio-environments is required to
25 better understand cellular mechanisms, search for novel therapeutic targets and design
26 optimal implants. Mechanisms of cell migration have been extensively studied *in vitro*
27 on two-dimensional (2D) surfaces, where it is described as a lamellipodia-based event
28 consisting mainly of 4 steps: extension of the leading edge, adhesion formation, traction
29 generation and subsequent retraction of the trailing edge [1]. So, cell migration on 2D
30 substrates is integrin-mediated and depends on the traction force cells exert on the
31 underlying material. Nevertheless cell migration has been shown to differ between the
32 traditional 2D models *in vitro* and the *in vivo* situations [2-5]. When switched to three-
33 dimensional (3D) culture systems - more representative of the *in vivo* environment -
34 different types of single cell migration can be described: (i) *mesenchymal migration*
35 which is proteolytic dependent and lamellipodia-based - and thus similar to 2D
36 migration (with implication of integrins and cell contractility) -; (ii) *amoeboid migration*
37 which is non-proteolytic dependent and where adhesions are inexistent or very weak [6-
38 8] and (iii) *lobopodia-based migration* which is determined by large cylindrical
39 protrusions and depends on the 3D matrix elasticity [9]. Additionally, cells of the same
40 type can switch between different modes of cell motility in response to the physical
41 properties of the environment, integrin impairment, degradability and soluble signalling
42 factors [9-12].

43

44 Given the difficulty of mimicking the *in vivo* nanoenvironment of the extracellular
45 matrix (ECM), different complex 3D culture systems have been used to study cell

46 migration [11, 13-15]. Unfortunately, differences inter- and even intra- 3D systems as
47 well as difficulties in having reliable 2D controls hinder identifying and understanding
48 the key features in 3D cell migration. Additional parameters play an important role in
49 3D migration such as (i) pore size [11], (ii) physical properties, e.g. matrix stiffness [9],
50 (iii) nutrients diffusion [16], (iv) degradability of the system [17], (v) topographical
51 cues [18], (vi) functionalities of the material (i.e. synthetic materials such as PEG
52 hydrogels should be modified with adhesion domains in order to permit cell adhesion)
53 [19] and (vii) variability of components from batch to batch [20]. Moreover, proper
54 quantitative methods for analysis of migration rates in 3D environments are still
55 lacking. New procedures to better understand cell migration within 3D cultures are
56 therefore needed.

57

58 The distribution of cell receptors anchored to the ECM within 3D microenvironments
59 highly differs from that observed on traditional 2D cultures. This is thought to be one of
60 the key causes for the different cell behaviour between 2D and 3D systems since
61 integrins trigger multiple signaling pathways which determine e.g. cell growth and gene
62 expression [21-23]. Furthermore, differences in integrin localization and expression
63 between 2D and 3D cultures have been described, supporting the hypothesis that
64 different outside-in signaling may be the cause of different cell behavior [2, 24].

65

66 We have previously observed that sandwich-like microenvironments provide dorsal
67 stimulation similar to 3D systems and trigger cell signaling pathways that promote a cell
68 behavior more similar to 3D environments [25-27]. Here, we hypothesize that the
69 excitation of dorsal receptors - by sandwiching cells already attached on a 2D surface -

70 might switch cell migration towards 3D modes. To assess this hypothesis, we studied
71 L929 fibroblast migration within sandwich-like cultures. Due to the high versatility of
72 the system, different well-controlled nanoenvironments can be explored to investigate
73 different parameters such as the protein conformation at the material interface. This
74 technology then becomes an interesting tool to study some specific aspects of cell
75 migration. In particular, we have varied the cell seeding procedure (culturing either
76 isolated cells or as in wound healing assays), the chemistry of the ventral surface (using
77 poly(ethyl acrylate), poly(methyl acrylate) and glass) and the biological input coming
78 from the dorsal substrate (coating samples with different proteins, e.g. fibronectin (FN)
79 and vitronectin (VN)) (see figure 1). Poly(lactic acid) (PLLA) was used as dorsal
80 substrate in all cases. Cell morphology, adhesion and migration under different culture
81 conditions were characterized, as well as the influence of the dorsal stimulation on the
82 ability of cells to remodel the ECM.

83

84 **Materials and methods**

85 **Materials**

86 Polymer films of ethyl acrylate and methyl acrylate (EA and MA respectively, Sigma-
87 Aldrich) were obtained by radical polymerization of a monomer solution using benzoin
88 (98% pure, Scharlau) as photoinitiator at 0,35 wt% and 1 wt% respectively. The
89 polymerization was carried out up to limiting conversion. Spin-coating was then used to
90 produce thin films of these polymers on glass coverslips (Brewer Science, Rolla, MO).
91 Polymer solutions were made in toluene with 2.5% PEA or 6% PMA and spin-coating
92 at 2000 rpm for 30 s. Finally, samples were dried at 60 °C in vacuum for 1 h before its
93 use as ventral substrates.

94 Thin films of PLLA were prepared by solvent casting a solution of 2% PLLA in
95 chloroform (Scharlau) in stainless steel washers and allowed to evaporate. Resulting
96 films were then thermally treated at 120 °C for 5 minutes and used as dorsal substrates.

97

98 **Protein adsorption**

99 Fibronectin from human plasma (FN; Sigma) at 20 µg/ml in DPBS, vitronectin at 10
100 µg/ml in DPBS (VN; Sigma) or heat-denatured Bovine Serum Albumin Fraction V
101 (BSA; Roche, Barcelona, Spain) at 10 mg/mL in MilliQ water were adsorbed on the
102 different substrates during 1 h at room temperature. After adsorption, samples were
103 rinsed in DPBS to eliminate the non-adsorbed protein.

104

105 **Atomic Force Microscopy**

106 Atomic force microscopy (AFM) was performed on a JPK Nanowizard 3 BioScience
107 AFM (JPK, Germany). Images were taken operating in the AC mode and analysed by
108 the SPM and DP 4.2 software version. Si-cantilevers with a force constant of 2.8 N/m
109 and a resonance frequency of 75 kHz (Nanoworld AG, Switzerland) were used. The
110 phase signal was set to zero at a frequency 5–10% lower than the resonance one. Drive
111 amplitude was 700 mV and the amplitude set point was 700 mV.

112

113 **Cell culture**

114 L929 fibroblasts were maintained in Dulbecco's Modified Eagle Medium (DMEM)
115 supplemented with 10% fetal bovine serum and 1% penicillin–streptomycin (Lonza).

116 Prior to seeding, samples were sterilized under UV for 30 min (30 min each side in the
117 case of the dorsal substrates) and coated as described before. Then L929 cells were
118 seeded in DMEM without serum in order to direct specific fibronectin-cell adhesion.
119 After 3 h of culture, sandwich cultures (SW) were obtained by gently laying the dorsal
120 substrate over the seeded ventral substrate where cells were already adhered (figure 1).
121 In order to better mimic SW conditions, a washer without PLLA was laid on the 2D
122 samples. Since several conditions have been studied, a specific nomenclature was used
123 overall the study: SW_x^y with x -ventral and y -dorsal material condition. More detailed
124 cell culture procedures can be found in the supplementary data.

125

126 **Time-lapse cell imaging**

127 Images were acquired every 20 min for 24 h using a Leica DMI 6000 inverted
128 microscope (Leica Microsystems) with a 10X dry objective. During the observation, the
129 samples were maintained at 37 °C and supplied with a 95% air and 5% CO₂ humidified
130 gas mixture. Phase contrast images were gathered at 20 min intervals along 24 h of
131 culture. For gap closure measurements, images were processed using the external plug-
132 in MiToBo in ImageJ software in order to obtain quantitative data about the dynamics
133 in cell migration [28, 29].

134

135 **Immunofluorescence**

136 Samples were fixed in 10% formalin solution (Sigma) at 4 °C for 30 min, “de-
137 sandwiched” and then permeabilised for 5 minutes. After that samples were incubated
138 in 1% BSA in order to reduce the background signal. Cells were then incubated with the

139 primary antibody (anti-vinculin and anti-paxilin antibodies (Sigma), anti-MMP2 and
140 anti-MMP13 (Abcam), anti- α -tubulin (Abcam), anti- β_1 integrin (BD Bioscience) or
141 anti- α_v integrin subunit (Millipore)) for 1 hour. Samples were then rinsed in DPBS/0.5%
142 Tween 20, followed by incubation with Cy3 or AlexaFluor 488 conjugated secondary
143 antibody (Jackson Immunoresearch and Invitrogen respectively). If necessary, samples
144 were incubated in BODIPY FL phalloidin (Molecular probes) diluted 1/100 in order to
145 stain the cytoskeleton. Finally the samples were washed before being mounted in
146 Vectashield containing 4',6-diamidino-2-phenylindole (DAPI, Atom).

147

148 **FN reorganization**

149 The ability of cells to reorganize the FN adsorbed on the ventral material surface was
150 evaluated after 7 h of culture. Samples were fixed, “de-sandwiched” and subjected to
151 FN immunodetection. The monoclonal primary antibody HFN7.1 that specifically binds
152 human FN III₉₋₁₀ domains was used (Developmental Studies Hybridoma Bank) to avoid
153 cross-reaction with FN secreted by murine cells.

154

155 **Image analysis**

156 Cell morphology was quantified by calculating different parameters using ImageJ
157 software. Cell area, aspect ratio (major axis/minor axis), circularity ($4 \pi \times$
158 $\text{area}/\text{perimeter}^2$) and roundness ($4 \times \text{area}/\pi \times [\text{major axis}]^2$) (the last 2 ones getting a
159 value of 1 for a perfect circle) were evaluated by analyzing at least 40 cells for each
160 condition [30]. Additionally, cell morphology and distribution of focal adhesions were
161 analyzed by The Focal Adhesion Analysis Server [31].

162

163 **Statistical analysis**

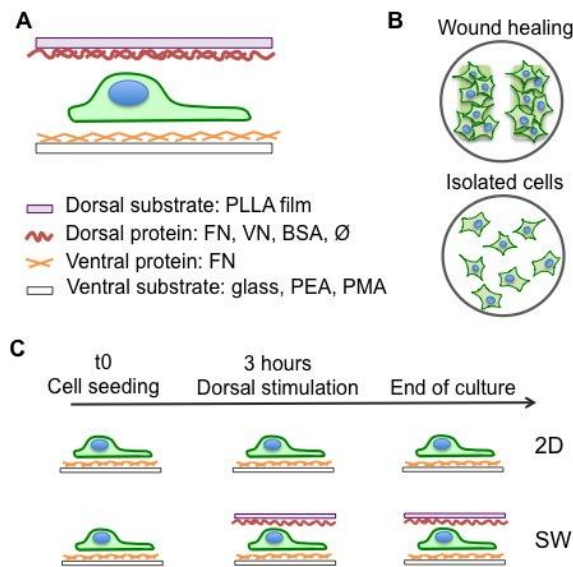
164 Results are shown as average \pm standard deviation. All experiments were performed at
165 least three times in triplicate. Results were analyzed by one-way ANOVA and if
166 significant differences were determined, Tukey's post-hoc test was performed. For each
167 sandwich condition, the bottom substrate as 2D culture was used as its specific control.
168 Statistically significant differences are indicated with * $P < 0.05$ and *** $P < 0.001$.

169

170 **Results and discussion**

171 **Phenomenology of cell migration within sandwich environments**

172 We have studied L929 fibroblasts migration within sandwich cultures using a modified
173 wound healing assay based on culture inserts since manual scratching stripped off the
174 thin spin-coated polymer films (figure 1). Moreover manual scratching of cell
175 monolayers has been correlated to changes in cell morphology, alteration of
176 proliferation and deregulation of migration [32].



177
178 Figure 1. Summary of the sandwich-like culture conditions. (A) Sketch of the sandwich-
179 like model and the different combinations of material and proteins. (B) Sketch of the
180 two different cell cultures used during this work. (C) Timing diagram showing the
181 procedure followed for sandwich culture systems.

182 Movie 1 (supplementary material) shows cell migration on FN coated glass coverslips
183 (2D) and then after overlying with a FN-coated PLLA film (sandwich culture, SW).
184 Cells on the 2D control migrate according to the classical 4 migration steps, by adopting
185 a polygonal shape with wide lamellipodia and pseudopodia projections [33, 34].
186 However, cells within sandwich culture adopted an elongated morphology with fewer
187 (usually 1 or 2) but longer pseudopodia that were more persistent in time resembling
188 what has been observed in other 3D environments (figure 2A) [9, 35, 36]. Such
189 elongated cell morphology of migrating cells has not been previously observed within
190 our sandwich microenvironments [25-27]. Importantly, also note that the nuclei of cells
191 migrating in sandwich environments hardly move from their initial position, which
192 suggests that the last steps of the migration process (traction generation and the
193 retraction of the trailing edge) were hindered or not coordinated [37].

194

195 One might think that the elongated morphology observed within the sandwich culture at
196 the front edge of the 2 cell populations in a wound healing assay might be related to the
197 biochemical crosstalk between the 2 populations (chemotaxis due to increased
198 concentration of cell secreted signals within the SW environment), which may enhance
199 extension directionality and persistence. However these elongated cells were observed
200 along the whole border of the seeded fields, not only the ones facing the wound. So we
201 first assessed whether this elongated morphology was due to the high cell density used
202 during the wound healing-like assay rather than to the specific sandwich condition.
203 Hence, isolated cells were cultured at low density and migration was monitored. Figure
204 2 depicts the morphology of selected cells after different time-points of culture so cell
205 morphology and migration can be evaluated. Cells overlaid with the FN-coated dorsal
206 substrate (sandwich culture, referred to as SW^{FN}) did not show such elongated
207 morphology. Hence the cause of this elongated morphology should be sought as a
208 consequence of combined dorsal stimuli and high cell density population, which
209 suggests an important role of cell-cell contact and Rac1 signaling [38]. To corroborate
210 this, high cell density areas of the wound healing were imaged and it was seen that only
211 cells in the periphery of the population projected the long pseudopodia whilst cells inside
212 the population conserved a polygonal shape (data not shown).

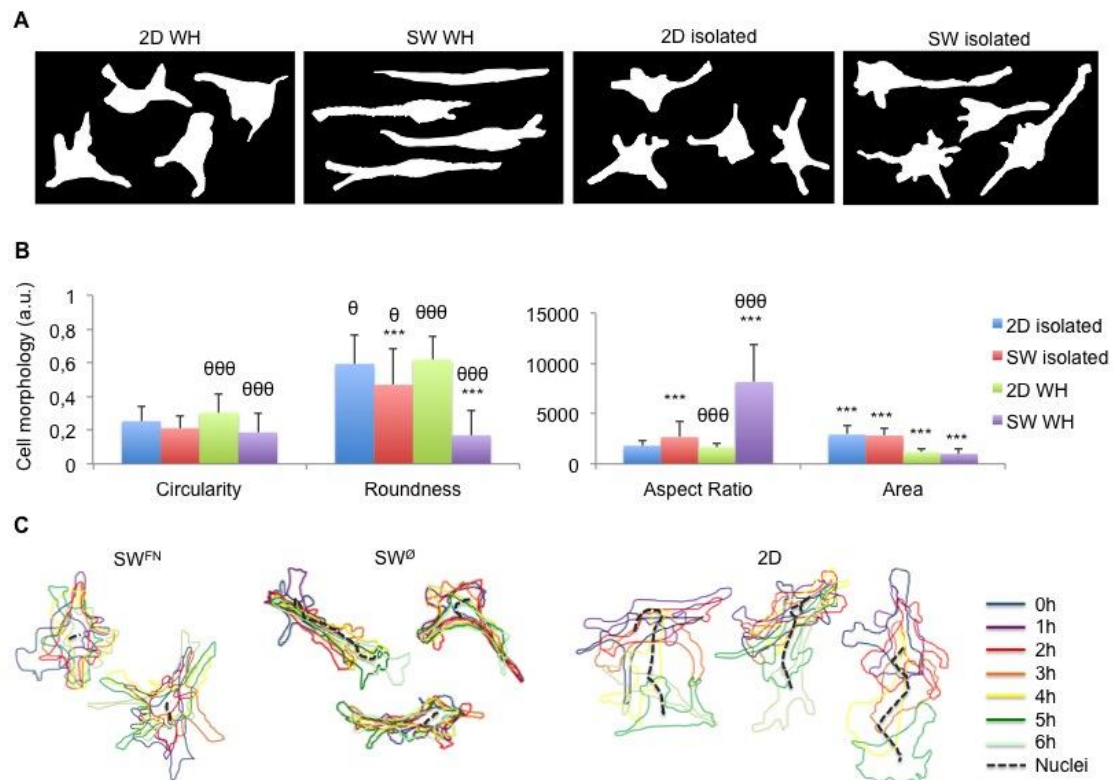
213

214 When the morphology of migrating cells within the sandwich culture was studied more
215 in depth (figure 2) we saw that the circularity of isolated cells was similar to the
216 circularity of cells during the wound healing assay (figure 2B) and, most importantly,
217 isolated cells within sandwich culture showed different roundness than isolated cells

218 cultured on 2D substrates. These suggest that, despite not having such long
219 pseudopodia, cells sense the dorsal stimuli and respond to it by changing their
220 morphology as reported for other 3D systems [39, 40]. Moreover, we have recently
221 shown that cell morphology within sandwich culture highly depends on the substrate
222 properties similarly as happens in 3D cultures [27]. Regarding cell motility, cells
223 cultured on 2D substrates moved around the starting point in random open trajectories,
224 whereas cells within SW^{FN} remain mainly static at the initial location, and only
225 cytoplasmatic extensions were projected (figure 2C). So, sandwich culture hinders cell
226 migration and nuclei movement both for isolated and wound healing cultures though
227 cells do project long pseudopodia only in the latter case.

228

229 In order to investigate the role of the nature of the dorsal stimulus, cells were studied
230 also when sandwiched with an un-coated dorsal substrate (SW^{\emptyset}). As a consequence
231 these cells received similar biological signals than cells on 2D samples, as the only
232 biologically driven interaction comes from the ventral substrate. As shown in figure 2C,
233 cells within SW^{\emptyset} can move and change their location, though less than on 2D
234 substrates. The lack of protein coating on the dorsal substrate is therefore related to an
235 increased cell migration compared to SW^{FN} , though cells do not behave as on the 2D
236 control. This suggests that not only the biological but also the mechanical stimuli are
237 important cues in sandwich environments [25-27].



238

239

Figure 2. Cell migration and morphology. (A) Cell morphology after 12 hours of

240

migration in a wound healing assay (WH) or as isolated cells (isolated). (B)

241

Morphology of cells after 12 hours of culture. * shows significance comparing isolated

242

with wound healing for the same type of dimensionality (2D or SW); and θ comparing

243

2D with SW for the same type of culture condition (isolated or wound healing). (C)

244

Outlined cells after different time points of culture. Dotted lines represent the movement

245

of cell nuclei. Coordinates are maintained for each outlined cell so that the displacement

246

displayed in the picture is equivalent to the migration observed during the culture.

247

248 **Characterization of the migrating cells**

249

Cells migrating in the wound healing assay were further characterized seeking to

250

understand differences with 2D conditions. Cultures were kept for 7 h to allow cells to

251

project these characteristic long pseudopodia within the sandwich culture. First, focal

252

adhesion proteins and integrins were evaluated as it is well accepted that these differ

253 between 2D and 3D/*in vivo* environments [2, 40-42]. Focal adhesion proteins such as
 254 pFAK^{Tyr925} and vinculin were detected at the cell edge when cultured on 2D substrates
 255 (figure 3). Within sandwich microenvironments, these proteins were localized mainly at
 256 the rear part of the cell and at the tip of the long pseudopodia. Besides, colocalization
 257 between vinculin and pFAK^{Tyr925} was observed in both conditions. Further differences
 258 between vinculin and pFAK did not only occur between both 2D and SW cultures but
 259 also when comparing the leading and rear part of cells migrating within the sandwich
 260 (table 1 and 2). Cells within the sandwich culture have a higher number of focal
 261 adhesions at the rear part than at the leading edge (table 1). This might explain why
 262 cells cannot retract the trailing edge during migration and only long pseudopodia are
 263 projected. Likewise, the larger focal adhesions observed for the sandwich culture (as
 264 well as the regulation of their turnover) might explain the lower migration rate [37, 43].

265

266

267

268 Table 1. pFAK and vinculin characterization in the leading and rear part of cells
 269 migrating within sandwich culture in a wound healing assay.

	Leading	Rear	P value
pFAK			
# Focal adhesions	165.11 ± 67.33	263 ± 90.8	< 0.0001 *
Area (μm ²)	1.06 ± 0.23	0.81 ± 0.18	< 0.0001 *
Total Area (μm ²)	164.47 ± 41.92	205.80 ± 58.07	0.0065 *
Distance to edge (μm)	1.83 ± 0.52	4.49 ± 1.01	< 0.001 *
Major axis (μm)	1.46 ± 0.2	1.29 ± 0.15	0.0019 *

Minor axis (μm)	0.79 \pm 0.09	0.68 \pm 0.06	< 0.0001 *
Vinculin			
# Focal adhesions	163.27 \pm 68.83	279.56 \pm 106.67	0.0012 *
Area (μm^2)	0.84 \pm 0.31	0.88 \pm 0.25	0.68
Total Area (μm^2)	133.56 \pm 65.62	234.45 \pm 71.45	0.0003 *
Major axis (μm)	1.36 \pm 0.28	1.41 \pm 0.21	0.54
Minor axis (μm)	0.67 \pm 0.11	0.71 \pm 0.10	0.30

270

271

272

273

274

275

276

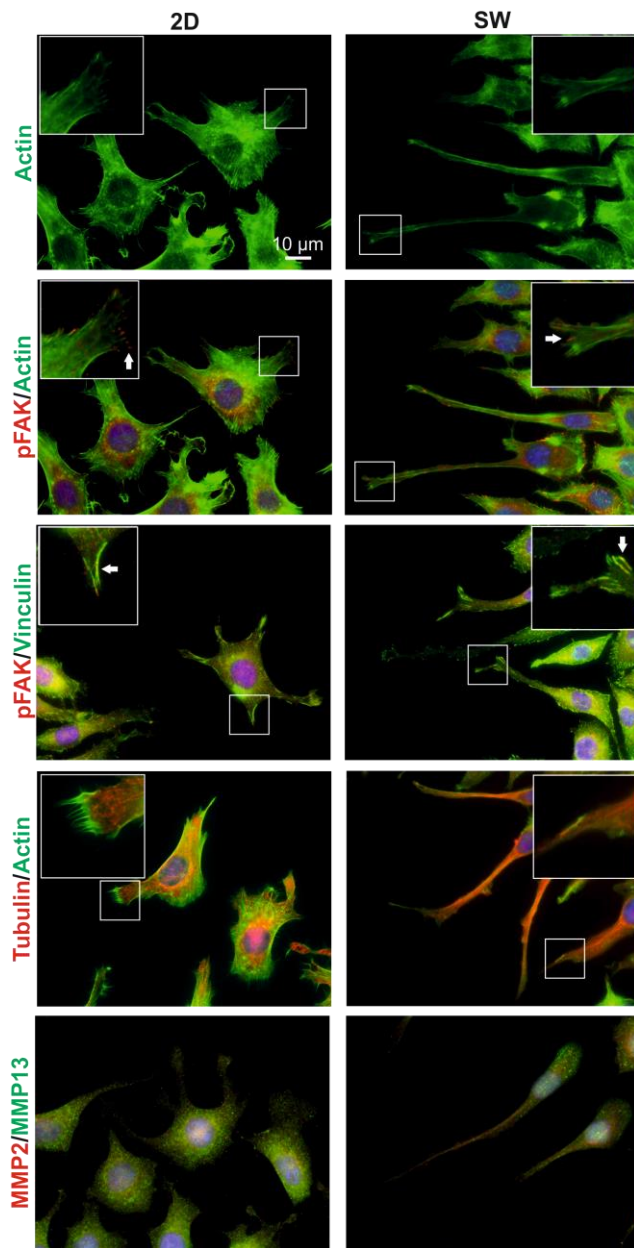
277

278 Table 2. pFAK and vinculin adhesions in 2D and sandwich cultures.

	2D	SW	P value
pFAK			
# Focal adhesions	682.22 \pm 193.64	382.75 \pm 98.31	0.0014 *
Area (μm^2)	0.57 \pm 0.05	0.69 \pm 0.14	0.0014 *
Total Area (μm^2)	387.31 \pm 100.69	258.33 \pm 64.95	0.0046 *
Distance to edge (μm)	6.39 \pm 1.56	3.56 \pm 0.89	0.0003 *
Major axis (μm)	1.03 \pm 0.03	1.20 \pm 0.14	< 0.0001 *
Minor axis (μm)	0.61 \pm 0.02	0.65 \pm 0.06	0.0154 *

Vinculin			
# Focal adhesions	495.44 ± 185.9	278 ± 114.29	0.0197 *
Area (μm^2)	0.74 ± 0.10	0.66 ± 0.09	0.59
Total Area (μm^2)	357.04 ± 102.95	240.05 ± 50.17	0.0108 *
Major axis (μm)	1.30 ± 0.11	1.33 ± 0.17	0.27
Minor axis (μm)	0.61 ± 0.03	0.64 ± 0.38	0.07

279



280

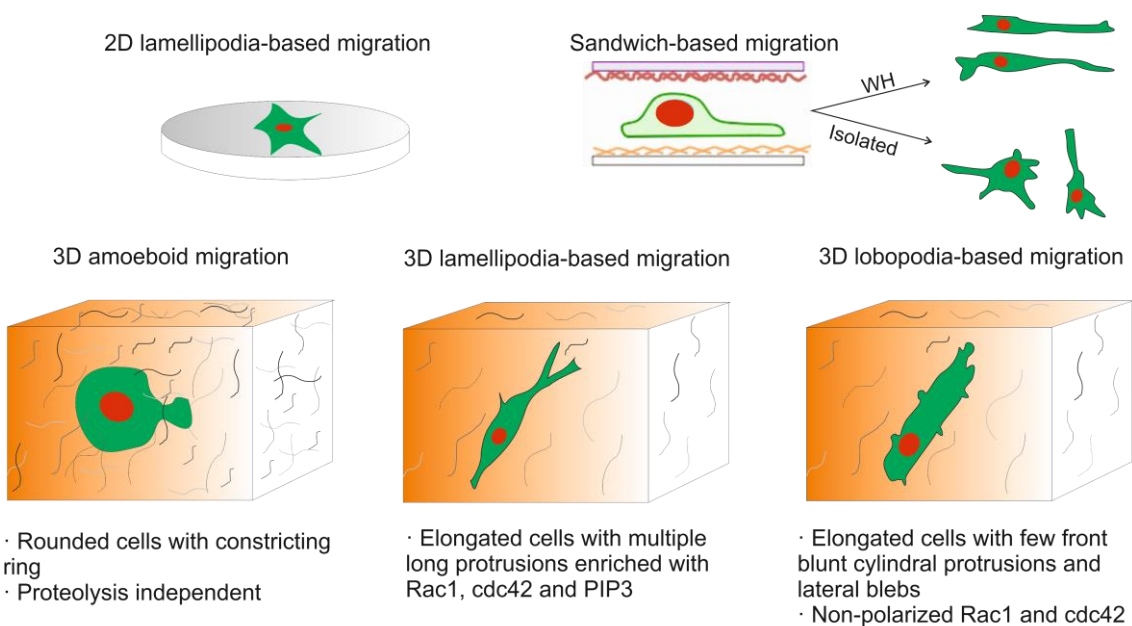
281 Figure 3. Immunofluorescence images after 7 hours of culture (2D and SW). Insets
282 show magnifications of focal adhesions and cell cytoskeleton. Arrows point out focal
283 adhesions.

284

285 Stressed actin fibers and developed α -tubulin microtubules were assembled both on 2D
286 and in SW cultures, but with different cell morphology that confined nuclei into a
287 narrower space within SW cultures. Likewise, broad actin lamellipodia were seen for
288 cells seeded on 2D substrates but not for cells within the sandwich culture (figure 3).
289 Similar elongated fibroblast morphology has been previously described for other 3D
290 systems. In particular, elongated cells with multiple long protrusions and small
291 lamellipodia at their tips (that contain Rac1, cortactin, PIP3 and Cdc42) have been
292 shown to use lamellipodia-based migration, whereas elongated cells with fewer
293 protrusions and no lamellipodia use the lobopodia-based migration. Interestingly, cells
294 switch between these 2 migration modes according to the elastic properties of the 3D
295 environment, which involve RhoA-ROCK-myosin II signalling [9]. Here we observe
296 elongated cells in SW with less lamellipodia than cells on 2D and without lateral blebs
297 (movie 1, figure 2 and figure 4), which corresponds to migration in a lamellipodia-based
298 mode. However, cells display only 1-2 protrusions at the leading edge, which might
299 suggest a new mode of migration mode for cells within SW environments intermediate
300 inbetween lamellipodia and lobopodia-based migration (figure 4). This is likely a
301 consequence of the environment provided by the sandwich system. Likewise, changing
302 the inputs coming from the sandwich environment could lead to different cell migration
303 (as in 3D systems [9]) similarly as it triggers differences in cell morphology, adhesion
304 and differentiation [25-27, 39].

305

306 ECM degradation is another key step for 3D cell migration [11, 9], as cells must
307 literally open spaces through the fibrillar mesh of proteins that constitute their
308 environment. We have investigated the expression of matrix metalloproteinases
309 (MMPs) – the main enzymes secreted by cells to degrade the ECM – and focused on
310 MMP2 and MMP13, that are known to degrade FN [44, 45]. However, no differences
311 were found for MMP2 and MMP13 on 2D and SW cultures (figure 3).



312

313 Figure 4. Schematic representation of cell migration modes in 2D, 3D and sandwich
314 culture. Differences in the migration mode are due to dimensionality, cell lineage and
315 ECM properties.

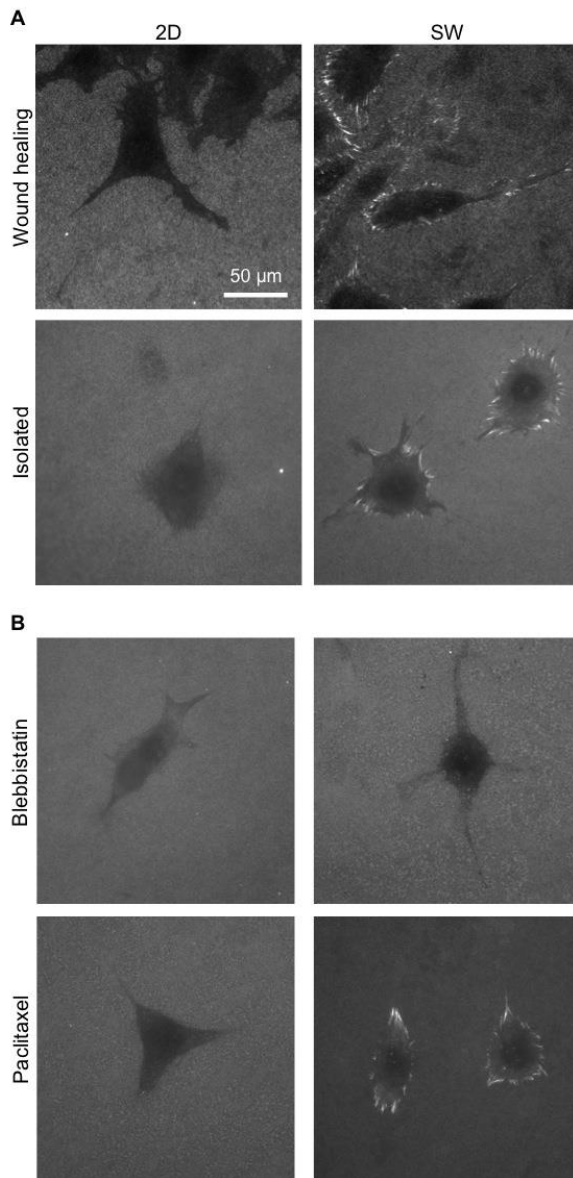
316

317 **Ventral ECM remodeling during cell migration**

318 It has been found that fibroblasts migrating in the lamellipodia mode remodel their
319 matrix but those in the lobopodia mode do not [9]. Hence, we investigated the role of

320 SW environments in ECM remodeling. The fate of ventral FN was studied on FN-
321 coated glass (2D) overlaid with a dorsal FN-coated PLLA film (SW). As a positive
322 control cells were cultured with growth medium (10% FBS) as this triggers ECM
323 reorganization [46]. It is important to remark here that for the rest of conditions cells
324 were cultured in serum-free medium, so that the sole influence of the sandwich
325 environment on cell reorganization was considered. Figure 5 shows that, regardless the
326 migration model used (wound healing or isolated cells), FN was not remodeled on 2D
327 substrates whilst cells formed new FN fibrils within sandwich cultures. Dorsal stimuli
328 did therefore trigger this ECM remodeling, as reported for FN and collagen in 3D
329 matrices [9, 47]. In order to better understand this phenomenon, we cultured cells in SW
330 under different dorsal conditions by coating with different proteins (vitronectin, bovine
331 serum albumin and un-coated; SW^{VN} , SW^{BSA} and SW^{\emptyset} respectively). As controls we
332 used 2D samples where the corresponding dorsal protein was included in the culture
333 medium, so that dorsal receptors were biologically but not mechanically stimulated. As
334 summarised in table 3, FN reorganization only occurred in sandwich cultures regardless
335 of the protein coating used, even occurring when the dorsal PLLA was coated with BSA
336 - SW^{BSA} (a non-adhesive protein) - or left uncoated (SW^{\emptyset}). Hence the mechanical dorsal
337 input has a key role to trigger FN reorganization and determine cell fate (figure 5 and
338 table 3).

339



340

341 Figure 5. Ventral FN reorganization. (A) Sandwich culture triggers ventral FN
 342 reorganization by forming new fibrils both in isolated and wound healing cultures. (B)
 343 Cell contractility is needed to reorganize FN within the sandwich culture.

344

345 Cell contractility is known to influence cell migration [9, 48, 49] via phosphorylation of
 346 myosin light chain (MLC) so we examined whether this might also be related to the
 347 ECM reorganization process triggered by SW environments. To do so cells were
 348 cultured in the presence of pharmacological inhibitors that impair contractility such as

349 the Rho/ROCK pathway inhibitor Y-27632 and Blebbistatin, a specific inhibitor of
 350 myosin II activity [50, 51]. In addition, cells were also cultured in the presence of
 351 Paclitaxel that stabilizes microtubules thus showing an opposite effect [52].
 352 Contractility inhibitors (Y-27632 and Blebbistatin) impaired the ventral FN
 353 reorganization within sandwich cultures whilst Paclitaxel enhanced it (figure 5B and
 354 table 3). Cell contractility is therefore needed to reorganize FN within the sandwich
 355 culture. Sandwich culture might therefore enhance cell contractility to enable the
 356 reorganization of ventral FN.

357

358 Table 3. Summary of the ventral FN reorganization. + stands for reorganization, - for no
 359 reorganization and * for the halo seen on PEA (see next section).

	2D	SW
Growth medium (+C)	+	+
Medium w/o serum	-	+
Blebbistatin/Y-27632	-	-
Paclitaxel	-	+
SW ^{FN/VN/BSA/Ø}		+
FN/VN/BSA dissolved in medium	-	
Ventral PEA/PMA	_*	-

360

361

362

363

364 **Role of the ventral substrate in cell migration**

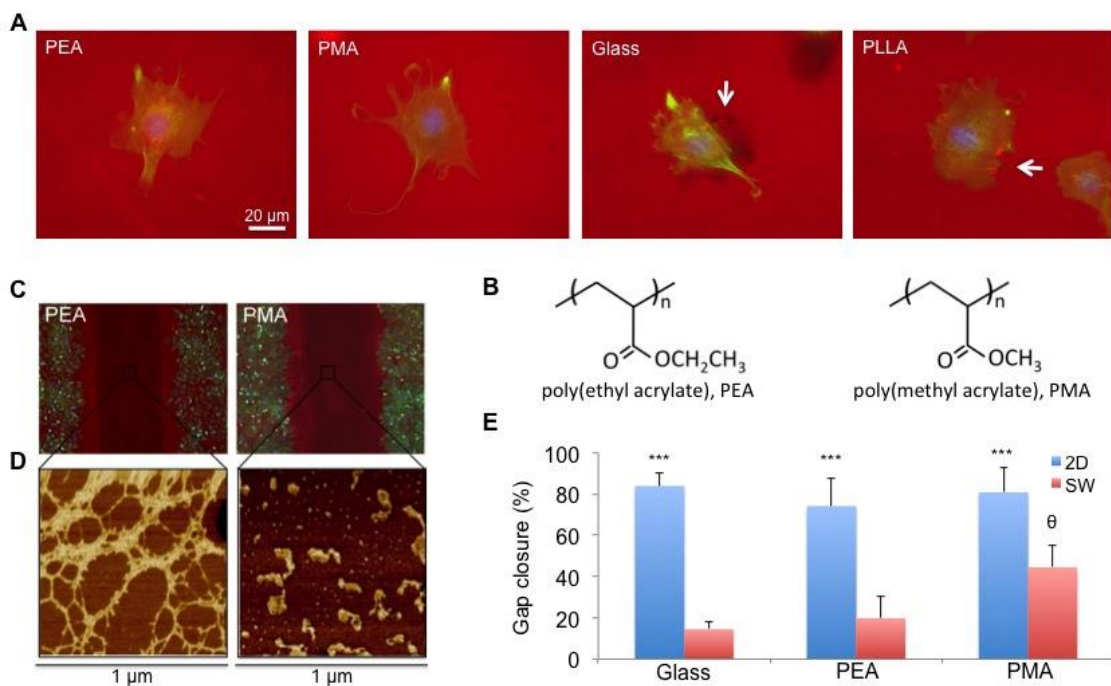
365 Next, we wanted to address if the elongated morphology and migration rates found for
366 migrating cells within SW environments might be tuned by using different materials as
367 ventral substrates. We used: (i) FN-coated glass, where FN adsorbs loosely in a globular
368 conformation that can be easily reorganized by cells [53], (ii) spin-coated poly(ethyl
369 acrylate) (PEA) on which FN assembles spontaneously into fibrillar (nano)networks
370 [54, 55] and (iii) spin-coated poly(methyl acrylate) (PMA) on which FN adopts a
371 globular conformation (figure 6) [56]. Figure 6A shows the cellular reorganization of
372 adsorbed FN after 5 h of culture (in growth media) on the different 2D substrates
373 (chemical structures shown in figure 6B). As expected, new FN fibrils were only
374 formed on glass and PLLA (white arrows) as cells are unable to reorganize FN on PEA
375 nor PMA due to the strength of the protein-material interactions [57]. Additionally we
376 addressed whether the ECM reorganization triggered by the dorsal stimuli in SW
377 cultures (using glass as ventral substrate) was also observed on PEA and PMA in the
378 absence of serum. Cells did not reorganize ventral FN on these surfaces, which suggests
379 that the dorsal stimulus is not strong enough to overcome the protein-material
380 interaction (table 3). Besides, FN showed a halo around cells when cultured on 2D PEA
381 substrates. This phenomenon has been further investigated and correlated with the
382 strength of FN-PEA interactions [58].

383

384 After assessing that removal of the culture insert did not alter the characteristic FN
385 adsorption and distribution on PEA and PMA (network and globular-like conformation
386 respectively; figure 6D), cell migration on the different materials was followed using
387 the wound healing assay. Gap closure, defined as the percentage of the initially void

388 surface that is colonized by cells, is shown in figure 6E. Polygonal cells were observed
 389 on every 2D substrate whilst cells adopted an elongated morphology when cultured
 390 under sandwich culture regardless of the material used. On the other hand, differences
 391 in cell migration were clearly observed between 2D and SW cultures for the same
 392 ventral substrate. Cells migrated longer distances on 2D substrates than within the SW
 393 environment, which increased gap closure (figure 6E). Finally, no differences in gap
 394 closure were observed for 2D samples but, strikingly, significant differences were
 395 observed for the different SW cultures: gap closure occurred more efficiently using
 396 PMA than glass or PEA, which suggests that FN conformation (globular on PMA and
 397 fibrillar structures on PEA) and the strength of FN interaction with the material surface
 398 play a key role in cell migration (figure 6E). Note that these differences appear only
 399 within SW environments but not for the 2D control, which stresses the role of
 400 dimensionality in cell migration.

401



402

403 Figure 6. Cell migration using different ventral FN-coated surfaces. (A) Fibronectin
404 (red) is reorganized on 2D glass and PLLA but not on PEA and PMA. Actin
405 cytoskeleton is shown in green and nuclei in blue. White arrows show the formation of
406 newly cell-reorganized FN fibrils. (B) Chemical structure of PEA and PMA. (C)
407 Fluorescence images show the FN-coated gap (500 μm) between the two cell
408 populations after removing the insert used for the wound healing assay. Actin
409 cytoskeleton (green), nuclei (blue) and FN (red) are shown. (D) AFM images of FN
410 after insert detachment to confirm that FN distribution is not altered on the migrating
411 area. (E) Gap closure after 24 h of wound healing assays using glass, PEA and PMA as
412 ventral substrates. * shows significance comparing conditions with similar ventral
413 substrate; and θ when comparing results of the same dimensionality (2D or SW).

414

415

416 **Role of dorsal stimuli in cell migration**

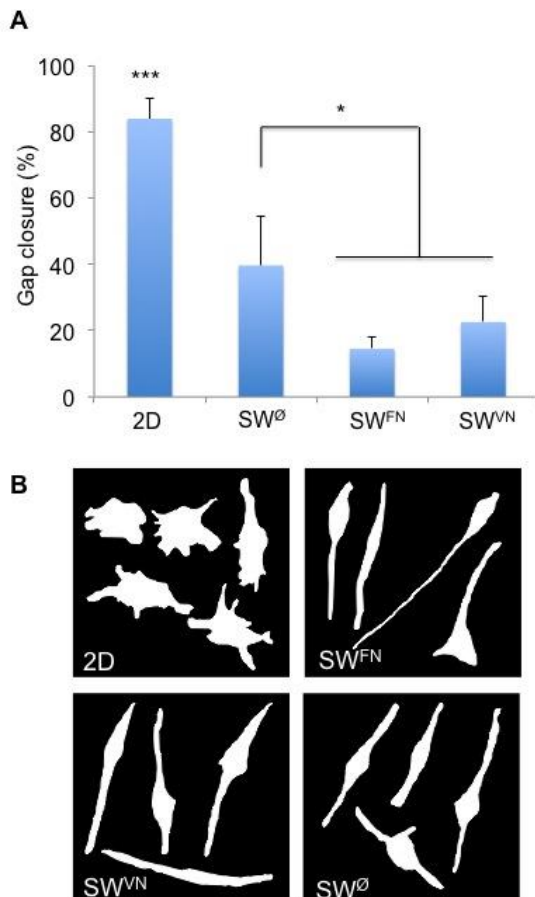
417 We next examined the role of dorsal stimuli in cell migration. To do so we used FN
418 coated glass as ventral substrate and as dorsal substrate (i) PLLA coated with different
419 proteins (FN or VN) to address the role of integrin-mediated interactions throughout
420 different proteins and (ii) bare surfaces (\emptyset) to address the effect of pure mechanical
421 stimuli (SW $^{\emptyset}$ might not induce any dorsal biological interaction but a response due to
422 the bare surface).

423

424 As observed previously, cells adopted polygonal morphology on 2D substrates and
425 elongated ones within sandwiched cultures. No differences in either gap closure or cell

426 morphology were observed regardless of the use of dorsal FN or VN coatings.
427 Strikingly, when overlaid by a non-adhesive dorsal substrate (SW^{\emptyset}), cells maintained
428 the characteristic elongated morphology found in SW cultures but migrated more
429 effectively (figure 7 and movie 2). So, even when the SW provided a pure mechanical
430 input (no protein coating), cell migration greatly differed. This observation, together
431 with results included in figure 2 and previous works [25], suggests an important role for
432 the dorsal mechanical input in cell behavior. Hence, we hypothesize that cell migration
433 is increased under this condition (SW^{\emptyset} ; both for isolated cells and wound healing assay)
434 compared with SW^{FN} and SW^{VN} due to the interactions with the extra (dorsal) layer of
435 proteins in the latter cases, and the regulation of focal adhesion formation and turnover
436 on both dorsal and ventral substrates.

437



438

439 Figure 7. Wound healing assay under different dorsal stimuli (2D and SW cultures) (A)
440 Migration rates after 24 hours of culture using FN-coated glass as ventral substrate and
441 bare PLLA (SW⁰) or coated with either FN or VN (SW^{FN} and SW^{VN} respectively) as
442 dorsal substrate. (B) Representative cell morphology of migrating cells for each
443 condition.

444

445 **Executive summary**

446 Background

- 447 • Cell migration is an essential process *in vivo*
- 448 • Robust culture systems mimicking the *in vivo* environment are needed

449 Results

- 450 • Sandwich culture offers a closer 3D environment and is a versatile system to
451 mimic different environments
- 452 • Cells sense and respond to the different ventral and dorsal stimuli in terms of
453 morphology, adhesion, ECM remodeling and migration rate
- 454 • Migration rates can be controlled by the ventral and dorsal stimuli provided by
455 sandwich environments

456

457 **Future perspective**

458 Cell migration is an essential process in many physiological and pathological
459 conditions. Providing novel tools to understand this process is therefore essential. Thus,
460 future work should develop more powerful and biomimetic systems and technologies to
461 investigate this process in *in vivo*-like conditions.

462 **Conclusions**

463 We have shown sandwich culture as a tool to investigate cell migration in a closer 3D
464 environment than the traditional 2D substrates. The versatility of this system allows the
465 study of cell fate under a wide spectrum of well-controlled conditions to better
466 understand cell behavior within 3D cultures such as stacked layers of cells or hydrogels.
467 Overall, cell morphology was highly influenced by the type of culture whereas cell
468 migration was determined by the inputs coming from both the ventral and dorsal
469 substrate. Furthermore, FN was reorganized in new fibrils when cells were dorsally
470 stimulated within the sandwich culture, showing that the dorsal excitation triggers
471 different signaling compared to 2D conditions. Our results suggest that both biological
472 and mechanical stimuli play an important role in cell migration.

473

474

475

476

477

478

479

480

481 **References**

482 1 Ridley AJ, Schwartz MA, Burridge K *et al.* Cell migration: integrating signals from
483 front to back. *Science*. 302(5651), 1704-1709 (2003).

484 2 Cukierman E, Pankov R, Stevens DR, Yamada KM. Taking cell-matrix adhesions to
485 the third dimension. *Science*. 294(5547), 1708-12 (2001).

486 *Characterization of adhesions in three-dimensional matrices

487 3 Lenaerts T, Castagnetti F, Traulsen A *et al.* Explaining the in vitro and in vivo
488 differences in leukemia therapy. *Cell Cycle*. 10(10), 1540-1544 (2011).

489 4 Zhang Z, Zhang ZY, Schluesener HJ. In vivo and in vitro differences between
490 leukocytic uptake of oligodeoxynucleotides. *Cell Mol Life Sci*. 65(7-8), 1237-1247
491 (2008).

492 5 Reig G, Pulgar E, Concha ML. Cell migration: from tissue culture to embryos.
493 *Development*. 141(10), 1999-2013 (2014).

494 6 Wolf K, Müller R, Borgmann S, Bröcker EB, Friedl P. Amoeboid shape change and
495 contact guidance: T-lymphocyte crawling through fibrillar collagen is independent of
496 matrix remodeling by MMPs and other proteases. *Blood*. 102(9), 3262-3269 (2003).

497 7 Friedl P. Prespecification and plasticity: shifting mechanisms of cell migration. *Curr*
498 *Opin Cell Biol*. 16(1), 14-23 (2004).

499 8 Wang W, Wyckoff JB, Frohlich VC, *et al.* Single cell behavior in metastatic primary
500 mammary tumors correlated with gene expression patterns revealed by molecular
501 profiling. *Cancer Res*. 62(21), 6278-6288 (2002).

502 9 Petrie RJ, Gavara N, Chadwick RS, Yamada KM. Nonpolarized signaling reveals two
503 distinct modes of 3D cell migration. *J Cell Biol*. 197(3), 439-55 (2012).

504 **Lamellipodia/lobopodia-based migration characterization

505 10 Sanz-Moreno V, Gaggioli C, Yeo M *et al.* ROCK and JAK1 signaling cooperate to
506 control actomyosin contractility in tumor cells and stroma. *Cancer Cell.* 20(2), 229-245
507 (2011).

508 11 Wolf K, Mazo I, Leung H *et al.* Compensation mechanism in tumor cell migration:
509 mesenchymal-amoeboid transition after blocking of pericellular proteolysis. *J Cell Biol.*
510 160(2), 267-277 (2003).

511 12 Friedl P, Wolf K. Plasticity of cell migration: a multiscale tuning model. *J Cell Biol.*
512 188(1), 11-9 (2010).

513 13 Schor SL, Ellis IR, Harada K *et al.* A novel 'sandwich' assay for quantifying chemo-
514 regulated cell migration within 3-dimensional matrices: wound healing cytokines
515 exhibit distinct motogenic activities compared to the transmembrane assay. *Cell Motil*
516 *Cytoskeleton.* 63(5), 287-300 (2006).

517 14 Lee EJ, Hwang CM, Baek DH, Lee SH. Fabrication of microfluidic system for the
518 assessment of cell migration on 3D micropatterned substrates. *Conf Proc IEEE Eng*
519 *Med Biol Soc.* 2009, 6034-6037 (2009).

520 15 Zaman MH, Trapani LM, Sieminski AL *et al.* Migration of tumor cells in 3D
521 matrices is governed by matrix stiffness along with cell-matrix adhesion and
522 proteolysis. *Proc Natl Acad Sci U S A.* 103(29), 10889-94 (2006).

523 16 Raghavan S, Shen CJ, Desai RA, Sniadecki NJ, Nelson CM, Chen CS. Decoupling
524 diffusional from dimensional control of signaling in 3D culture reveals a role for
525 myosin in tubulogenesis. *J Cell Sci.* 123(Pt 17), 2877-2883 (2010).

526 17 Lee SH, Miller JS, Moon JJ, West JL. Proteolytically degradable hydrogels with a
527 fluorogenic substrate for studies of cellular proteolytic activity and migration.
528 *Biotechnol Prog.* 21(6), 1736-1741 (2005).

529 18 Sundararaghavan HG, Saunders RL, Hammer DA, Burdick JA. Fiber alignment
530 directs cell motility over chemotactic gradients. *Biotechnol Bioeng.* 110(4), 1249-1254
531 (2013).

532 19 Raeber GP, Lutolf MP, Hubbell JA. Molecularly engineered PEG hydrogels: a novel
533 model system for proteolytically mediated cell migration. *Biophys J.* 89(2), 1374-1388
534 (2005).

535 20 Hughes CS, Postovit LM, Lajoie GA. Matrigel: a complex protein mixture required
536 for optimal growth of cell culture. *Proteomics.* 10(9), 1886-1890 (2010).

537 21 Hynes RO. Integrins: bidirectional, allosteric signaling machines. *Cell.* 110(6), 673-
538 687 (2002).

539 22 Burridge K, Chrzanowska-Wodnicka M. Focal adhesions, contractility, and
540 signaling. *Annu Rev Cell Dev Biol.* 12, 463-518 (1996).

541 23 Schwartz MA, Ginsberg MH. Networks and crosstalk: integrin signalling spreads.
542 *Nat Cell Biol.* 4(4), E65-8 (2002).

543 24 Moghe PV, Ezzell RM, Toner M, Tompkins RG, Martin LY. Role of β 1 Integrin
544 Distribution in Morphology and Function of Collagen-Sandwiched Hepatocytes. *Tissue*
545 *Engineering*, 3(1), 1-16 (1997)

546 25 Ballester-Beltrán J, Lebourg M, Rico P, Salmerón-Sánchez M. Dorsal and ventral
547 stimuli in cell-material interactions: effect on cell morphology. *Biointerphases*. 7(1-4),
548 39 (2012).

549 26 Ballester-Beltrán J, Lebourg M, Salmerón-Sánchez M. Dorsal and ventral stimuli in
550 sandwich-like microenvironments. Effect on cell differentiation. *Biotechnol Bioeng*.
551 110(11), 3048-3058 (2013).

552 27 Ballester-Beltrán J, Moratal D, Lebourg M, Salmerón-Sánchez M. Fibronectin-
553 matrix sandwich-like microenvironments to manipulate cell fate. *Biomater Sci*. 2, 381-
554 389 (2014).

555 *Importance of sandwich culture conditions for cell behavior

556 28 Rasband WS. ImageJ U.S. National Institutes of Health, Bethesda, Maryland, USA,
557 <http://imagej.nih.gov/ij/1997-2012>

558 29 Glaß M, Möller B, Zirkel A *et al*. Cell Migration Analysis: Segmenting Scratch
559 Assay Images with Level Sets and Support Vector Machines. *Pattern Recognition*.
560 45(9), 3154-3165 (2012).

561 30 O'Connell B. Oval Profile Plot. Research Services Branch, National Institute of
562 Mental Health, National Institute of Neurological Disorders and Stroke. Available from:
563 <http://rsbweb.nih.gov/ij/plugins/oval-profile.html>. Accessed 20 March 2014.

564 31 Berginski ME, Gomez SM. The Focal Adhesion Analysis Server: a web tool for
565 analyzing focal adhesion dynamics. *F1000Research* (2), 68 (2013).
566 <http://faas.bme.unc.edu> Accessed July 2014.

567 32 Kam Y, Guess C, Estrada L, Weidow B, Quaranta V. A novel circular invasion assay
568 mimics in vivo invasive behavior of cancer cell lines and distinguishes single-cell
569 motility in vitro. *BMC Cancer*. (8), 198 (2008).

570 33 Lauffenburger DA, Horwitz AF. Cell migration: a physically integrated molecular
571 process. *Cell*. 84(3), 359-369 (1996).

572 34 Ridley AJ, Schwartz MA, Burridge K *et al*. Cell migration: integrating signals from
573 front to back. *Science*. 302(5651), 1704-1709 (2003).

574 35 Decaestecker C, Debeir O, Van Ham P, Kiss R. Can anti-migratory drugs be
575 screened in vitro? A review of 2D and 3D assays for the quantitative analysis of cell
576 migration. *Med Res Rev*. 27(2), 149-176 (2007).

577 36 Fraley SI, Feng Y, Krishnamurthy R *et al*. A distinctive role for focal adhesion
578 proteins in three-dimensional cell motility. *Nat Cell Biol*. 12(6), 598-604 (2010).

579 37 Nagano M, Hoshino D, Koshikawa N, Akizawa T, Seiki M. Turnover of focal
580 adhesions and cancer cell migration. *Int J Cell Biol*. 2012, 310616 (2012)

581 38 Pankov R, Endo Y, Even-Ram S *et al*. A Rac switch regulates random versus
582 directionally persistent cell migration. *J Cell Biol*. 170(5), 793-802 (2005).

583 39 Beningo KA, Dembo M, Wang YL. Responses of fibroblasts to anchorage of dorsal
584 extracellular matrix receptors. *Proc Natl Acad Sci U S A*. 101(52), 18024-18029 (2004).

585 **Cell behavior under polyactylamide sandwich cultures

586 40 Hakkinen KM, Harunaga JS, Doyle AD, Yamada KM. Direct comparisons of the
587 morphology, migration, cell adhesions, and actin cytoskeleton of fibroblasts in four

588 different three-dimensional extracellular matrices. *Tissue Eng Part A*. 17(5-6), 713-724
589 (2011).

590 **Deep study of cell migration in 3D systems

591 41 Ochsner M, Textor M, Vogel V, Smith ML. Dimensionality controls cytoskeleton
592 assembly and metabolism of fibroblast cells in response to rigidity and shape. *PLoS*
593 *One*. 5(3), e9445 (2010).

594 42 Harunaga JS, Yamada KM. Cell-matrix adhesions in 3D. *Matrix Biol*. 30(7-8), 363-
595 368 (2011).

596 43 Kim DH, Wirtz D. Focal adhesion size uniquely predicts cell migration. *FASEB J*.
597 27(4), 1351-1361 (2013).

598 44 Collier IE, Wilhelm SM, Eisen AZ *et al*. H-ras oncogene-transformed human
599 bronchial epithelial cells (TBE-1) secrete a single metalloprotease capable of degrading
600 basement membrane collagen. *J Biol Chem*. 263(14), 6579-6587 (1988).

601 45 Knäuper V, Cowell S, Smith B *et al*. The role of the C-terminal domain of human
602 collagenase-3 (MMP-13) in the activation of procollagenase-3, substrate specificity, and
603 tissue inhibitor of metalloproteinase interaction. *J Biol Chem*. 272(12), 7608-7616
604 (1997).

605 46 Gugutkov D, Altankov G, Rodríguez Hernández JC, Monleón Pradas M, Salmerón
606 Sánchez M. Fibronectin activity on substrates with controlled --OH density. *J Biomed*
607 *Mater Res A*. 92(1), 322-31 (2010).

608 47 Mao Y, Schwarzbauer JE. Stimulatory effects of a three-dimensional
609 microenvironment on cell-mediated fibronectin fibrillogenesis. *J Cell Sci.* 118(Pt 19),
610 4427-4436 (2005).

611 48 Roca-Cusachs P, Iskratsch T, Sheetz MP. Finding the weakest link: exploring
612 integrin-mediated mechanical molecular pathways. *J Cell Sci.* 125(Pt 13), 3025-3038
613 (2012).

614 49 Doyle AD, Wang FW, Matsumoto K, Yamada KM. One-dimensional topography
615 underlies three-dimensional fibrillar cell migration. *J Cell Biol.* 184(4), 481-490 (2009).

616 50 Narumiya S, Ishizaki T, Uehata M. Use and properties of ROCK-specific inhibitor
617 Y-27632. *Methods Enzymol.* 325:273-284 (2000).

618 51 Kovács M, Tóth J, Hetényi C, Málnási-Csizmadia A, Sellers JR. Mechanism of
619 blebbistatin inhibition of myosin II. *J Biol Chem.* 279(34):35557-35563 (2004).

620 52 Fitzpatrick FA, Wheeler R. The immunopharmacology of paclitaxel (Taxol),
621 docetaxel (Taxotere), and related agents. *Int Immunopharmacol.* 3(13-14):1699-1714
622 (2003).

623 53 Ballester-Beltrán J, Rico P, Moratal D, Song W, Mano JF, Salmerón-Sánchez M.
624 Role of superhydrophobicity in the biological activity of fibronectin at the cell–material
625 interface. *Soft Matter.* (7), 10803-10811 (2011)

626 54 Rico P, Rodríguez Hernández JC, Moratal D *et al.* Substrate-induced assembly of
627 fibronectin into networks: influence of surface chemistry and effect on osteoblast
628 adhesion. *Tissue Eng Part A.* 15(11), 3271-3281 (2009).

629 *Different fibronectin adsorption on similar substrates

630 55 Ballester-Beltrán J, Cantini M, Lebourg M *et al.* Effect of topological cues on
631 material-driven fibronectin fibrillogenesis and cell differentiation. *J Mater Sci Mater*
632 *Med.* 23(1), 195-204 (2012).

633 56 Salmerón-Sánchez M, Rico P, Moratal D, Lee TT, Schwarzbauer JE, García AJ.
634 Role of material-driven fibronectin fibrillogenesis in cell differentiation. *Biomaterials.*
635 32(8), 2099-2105 (2011).

636 57 Llopis-Hernández V, Rico P, Moratal D, Altankov G, Salmerón-Sánchez M. Role of
637 material-driven fibronectin fibrillogenesis in protein remodeling. *Biores Open Access.*
638 2(5), 364-373 (2013).

639 58 Gonzalez-Garcia C, Cantini M, Ballester-Beltran J, Salmeron-Sanchez M. Nanoscale
640 mobility of fibronectin at the material interface determines cell fate. *Submitted*

641